

Changes in physical properties of tropical and temperate hardwoods below and above the fiber saturation point

G. Almeida · R. E. Hernández

Received: 12 October 2005 / Published online: 17 May 2006
© Springer-Verlag 2006

Abstract Changes in physical and mechanical properties of wood were analyzed using sorption tests combined with dimensional measurements and perpendicular-to-the-grain tangential compression tests. In order to determine the influence of wood structure on these changes, three hardwood species (*Fagus grandifolia*, *Brosimum alicastrum* and *Cariniana domestica*) presenting different anatomical structures were studied. Two experimental techniques were used to perform moisture sorption tests at 25°C. The first technique used saturated salt solutions (from 33 to 90% relative humidity) and the second used the pressure membrane method (above 96% relative humidity). Special attention was given to the “fiber saturation region”, where changes in wood properties started to take place. Results showed that at equilibrium moisture content (EMC), radial, tangential and volumetric shrinkage, as well as changes in transverse strength occurred above the fiber saturation point (FSP). This behavior can be explained by the effect of hysteresis at saturation on wood properties. This hysteresis indicates that loss of bound water takes place in the presence of liquid or capillary water, which contradicts the concept of FSP. The initial EMC at which bound water starts to be removed varied largely among the wood species.

G. Almeida (✉) · R. E. Hernández
Centre de recherche sur le bois (CRB),
Département des sciences du bois et de la forêt,
Université Laval Québec, QC, Canada G1K 7P4
e-mail: giana.almeida.1@ulaval.ca

R. E. Hernández
e-mail: roger.hernandez@sbf.ulaval.ca

Introduction and background

The physical and mechanical behavior of wood as a hygroscopic material needs to be fully understood in order to improve its utilization. The fiber saturation point (FSP) is a very important concept in the study of the influence of moisture content (MC) on the physical and mechanical properties of wood. The FSP was initially defined by Tiemann (1906) as the MC at which the cell walls are saturated with bound water with no free water in the cell cavities. It is normally assumed that the FSP is the MC below which the physical and mechanical properties of wood begin to change as a function of MC (USDA 1974; Siau 1984). Therefore, the FSP is used in models to adjust the mechanical properties of wood as a function of its MC (Bodig and Jayne 1982), as well as in wood shrinkage and density adjustment models (Siau 1984; Skaar 1988).

However, some results reported in the literature show that this assumption may not be realistic. Stevens (1963) found that shrinkage in beech begins to take place above the FSP. He suggested an MC gradient effect for explaining this behavior, but this hypothesis appears to be incompatible with the fact that shrinkage values reported in this study were measured at the equilibrium moisture content (EMC). Barkas (1938) measured changes in dimensions of small wood samples, where the presence of MC gradient is virtually negligible. He concluded that shrinkage in beech wood existed at moisture contents far above the FSP. Goulet and Hernández (1991) reported a large hysteresis effect on the EMC and on the perpendicular-to-the-grain tangential tension strength of sugar maple wood at high relative humidities (RH). The difference for the tangential tension strength between adsorption and desorption states was 20% at 26% EMC. This effect was attributed to the hysteresis at saturation phenomenon, which affected the wood moisture sorption above 63% RH (Hernández 1983). This hysteresis implies that during desorption the loss of bound water begins before all liquid water has been removed from the wood.

Even though desorption curves showed 26% EMC as an upper limit, Goulet and Hernández (1991) predicted that the effect of MC on sugar maple wood properties could be extended beyond the FSP, estimated to be 31% MC. Two studies focusing on high humidities (above 90% RH) were, therefore, conducted on sugar maple (Hernández and Bizoň 1994) and yellow birch woods (Almeida and Hernández 2006a). The results demonstrated that at the EMC, changes in transverse and volumetric shrinkage, as well as changes in transverse strength, occur above the FSP for both species. The initial EMC at which bound water starts to be removed from wood was 42.5% for sugar maple and about 41% EMC for yellow birch. This occurs even with the presence of liquid water within the wood structure. The results of Hernández and Bizoň (1994) were outlined later by Siau (1995) when describing the FSP. More research on wood species presenting different wood structures is needed in order to further develop these conclusions.

The main objective of this investigation was therefore to study the effect of EMC on wood properties of tropical and temperate hardwoods below and above the cell-wall saturation. Two moisture sorption techniques using saturated salt solutions (between 33 and 90% RH) and the pressure membrane method (above 96% RH) were applied to large samples at 25°C. These sorption tests were combined with shrinkage measurements as well as perpendicular-to-the-grain tangential compression tests.

Materials and methods

The experiments were carried out with one temperate hardwood: beech (*Fagus grandifolia* Ehrhart); and two tropical hardwoods: congona (*Brosimum alicastrum* Swartz) and cachimbo (*Cariniana domestica* (*C. martius*) Miers). The specimens for physical and mechanical tests had a cross-section of 20 mm (*R*) by 20 mm (*L*) and a height of 60 mm (*T*). Additional matched samples were used to study the anatomical structure of these hardwood species. A more detailed description of the longitudinal matching, the conditioning of the wood specimens and the anatomical tests can be found in Almeida and Hernández (2006a, b).

The average basic wood density (oven-dry mass to green volume) of the three species studied was 543 kg m⁻³ for beech (coefficient of variation (CV) of 3%); 540 kg m⁻³ for congona (CV of 4%) and 550 kg m⁻³ for cachimbo (CV of 5%).

Experiments

The experiments consisted of moisture sorption tests associated with shrinkage and mechanical tests. Wood specimens were mechanically tested as soon as the desired EMC was reached. The sorption conditions studied are shown in Table 1. Prior to the desorption tests, specimens were saturated in three steps until their full moisture content was reached. This was done in order to avoid internal defects caused by a rapid moisture adsorption (Naderi and Hernández 1997). The full saturated masses were then determined to the nearest 0.001 g using a digital balance and dimensions in all principal directions to the nearest 0.001 mm were measured with a digital micrometer. The group to be conditioned in adsorption over distilled water was kept at 20°C and 60% RH prior to the adsorption test.

The sorption experiments required two experimental techniques. The first technique involved the use of saturated salt solutions. The second one conditioned specimens by employing a pressure membrane procedure. A detailed description of these techniques was given previously by Almeida and Hernández (2006a). For the saturated salt solutions, the time of conditioning varied between 124 days (congona and cachimbo in desorption at 58% RH) and 419 days (beech in desorption at 90% RH). For each point of sorption, control specimens were weighed periodically, without being removed from the

Table 1 Characteristics of the moisture sorption conditions used in these experiments

State of sorption	Chemical or saturated salt solution	Nominal relative humidity (%)	Water potential (J kg ⁻¹)	Radius of curvature of the air–water meniscus ^a (μm)
<i>Full saturation under distilled water</i>				
Saturation ^b	H ₂ O	100	0	∞
<i>Equilibrium under a pressure membrane at 25°C</i>				
Desorption ^c	–	99.989	–15	9.60
Desorption ^b	–	99.927	–100	1.44
Desorption ^d	–	99.782	–300	0.480
Desorption ^c	–	99.637	–500	0.288
Desorption ^d	–	99.492	–700	0.206
Desorption ^b	–	98.557	–2,000	0.072
Desorption ^c	–	96.782	–4,500	0.032
Desorption ^d	–	96.431	–5,000	0.029
<i>Equilibration over saturated salt solutions at 25°C</i>				
Adsorption ^b	H ₂ O	≈ 100	–	–
Desorption ^b	ZnSO ₄	90	–14,495	–
Desorption ^b	KCl	86	–20,750	–
Desorption ^b	NaCl	76	–37,756	–
Desorption ^b	NaBr	58	–74,941	–
Desorption ^b	MgCl ₂	33	–152,526	–

^a $r = (-2\gamma \cos \theta) / \psi$; where γ is the surface tension of water (0.072 N m⁻¹ at 25°C) and θ the contact angle between the liquid and the surface of the capillary (0°). Under about 92% RH, equation is not applicable

^bSorption condition tested on the three species

^cSorption condition tested on beech

^dSorption condition tested on congona and cachimbo

desiccator. It was assumed that the EMC was reached when the loss (desorption) or gain (adsorption) in MC was at least less than 0.007% MC per day.

The pressure membrane procedure was used to determine additional points of desorption between 96.431 and 99.989% RH (Table 1). This technique is suitable for this humidity range and has been used by many researchers before (Stone and Scallan 1967; Griffin 1977; Fortin 1979; Hernández and Bizoñ 1994; Almeida and Hernández 2006a). The procedure introduces the concept of water potential (ψ), which is derived from classical thermodynamics and is defined as the difference between the specific Gibbs free energies of water in the state under study and in a standard reference state (Siau 1995). A detailed description of the apparatus used for the pressure membrane method is given by Cloutier and Fortin (1991). For each point of longitudinal desorption, 20 saturated specimens were placed into the pressure extractor on a saturated cellulose acetate membrane. Pressure was then gradually applied until the required level was reached. Flow of water was collected in a burette. EMC was considered as reached when outflow became negligible (no outflow during seven successive days). The desorption phase required between 3 and 90 days, depending on the ψ considered and the wood species tested.

As soon as each sorption test was completed, the sample mass was measured to the nearest 0.001 g. Dimensions in all principal directions were taken to the nearest 0.001 mm with a micrometer. Tangential compression tests were immediately carried out on a Riehle machine (beech) and on a MTS Q Test/5 machine (cachimbo and congona) equipped with an appropriate load cell. The strain was measured over a span of 40 mm on the central part of the specimen, using a two-side clip gauge provided with a Sangamo DG 1.0 linear displacement sensor (LVDT). In addition, the entire deformation of the specimen was measured by the displacement of the crosshead, using another Sangamo LVDT in the case of beech samples or using the data given by the machine in the case of cachimbo and congona samples. Hygrothermal changes during all mechanical tests were controlled by wrapping specimens in cotton that had been previously conditioned above the same humidity conditions as the wood. As per Sliker (1978), the crosshead speed was adjusted in order to ensure a similar strain rate for all moisture conditions. In the elastic range this strain rate was $0.01 \text{ mm mm}^{-1} \text{ min}^{-1}$.

In addition to the sorption experiments, a group of samples that had been fully saturated with distilled water was mechanically tested. This was done in order to compare the properties measured under this condition with those evaluated from the group conditioned over distilled water.

The test results were used to calculate the compliance coefficient in the tangential direction (s_{33}) of the wood. The reciprocal of this parameter is Young's modulus. Strain–stress curves were plotted using consecutive strain–stress readings recorded by a data acquisition system. Stress at the proportional limit was defined as where the recorded strain differed by 1% of that estimated by a linear regression analysis using all lower strain readings obtained within the elastic range of the curve. The cross-sectional area used for the calculations was that measured at the time of testing. Differences in dimensions of specimens after full moisture saturation and before the mechanical test were used to estimate partial percent shrinkage in the tangential (β_{TH}) and radial (β_{RH}) directions of the wood. Volumetric shrinkage was estimated to be the summation of these two directional shrinkages ($\beta_{\text{TH}} + \beta_{\text{RH}} - \beta_{\text{TH}} \cdot \beta_{\text{RH}}$). The mass of the specimens just before the mechanical test and their mass measured after oven-drying were used to calculate the EMC, expressed as a percentage of oven-dry mass.

Results and discussion

Wood hygroscopicity

The relationship between water potential and EMC for the three hardwoods is given in Fig. 1. This figure only displays the desorption curve obtained by using either the pressure membrane or the saturated salt solution methods. An excellent continuity is apparent between the results obtained by both sorption methods. This confirms the suitability of the pressure membrane method for

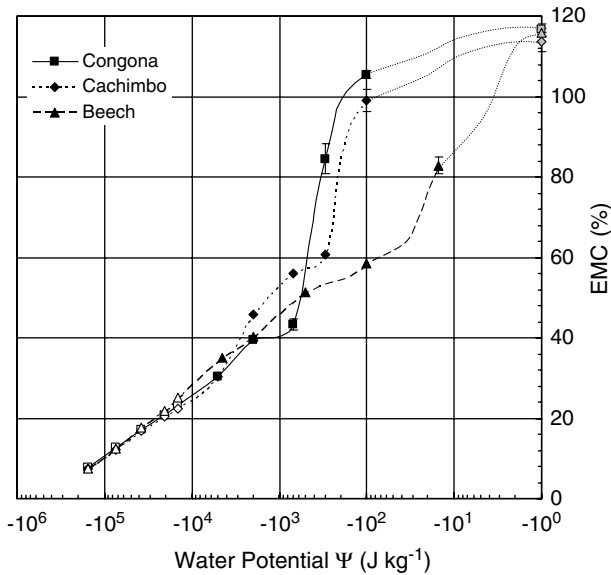


Fig. 1 Equilibrium moisture content as a function of the water potential of beech, congona and cachimbo hardwoods at 25°C. *Gray symbols* represent full saturation under distilled water; *black symbols* are the values obtained by the pressure membrane method and *white symbols* are the values obtained with the saturated salt solution method (standard errors are shown only when they exceed the symbol size)

determining EMC in wood under high relative humidity conditions, which is consistent with several earlier reports (Stone and Scallan 1967; Griffin 1977; Cloutier and Fortin 1991; Hernández and Bizoñ 1994; Defo et al. 1999; Almeida and Hernández 2006a).

In this study, desorption was carried out beginning from the fully saturated state, and the curve obtained corresponds to the maximum EMC expected for each humidity condition. The term boundary desorption curve is therefore used to describe this feature. Any desorption curve obtained from a lower initial MC would be located below this boundary desorption curve (Defo et al. 1999).

The region between 96 and 100% RH (ψ higher than -10^4 J kg $^{-1}$) is greatly expanded when using the water potential concept to represent sorption isotherms. This region is very important when studying the wood–water interactions given that they are mainly controlled by the capillary forces and consequently by the microstructure of wood species. Since wood is a porous material, an important effect to be considered in the interpretation of Fig. 1 is the “ink-bottle effect”. The capillary system of wood consists of cavities interconnected by narrow channels. The variation in dimensions between the different types of cavities connected in series suggests that desorption tends to be governed by a lower water potential, which is determined by the narrower sections of the pores. In contrast, adsorption tends to be governed by a higher water potential that depends on the larger sections of the pores. Thus, the

desorption isotherm will depend on the size of channels connecting the lumina, whereas the adsorption isotherm will depend on the size of these lumina (Fortin 1979).

The anatomical structure of beech wood is very different from that of congona and cachimbo woods. The temperate species has a large amount of vessel elements with a minute dimension (Almeida and Hernández 2006b). The boundary desorption curve (Fig. 1) shows that at $-100 \text{ J kg}^{-1} \psi$ beech wood had already lost 57% MC. In order to obtain more EMC values between full saturation and $-100 \text{ J kg}^{-1} \psi$, a supplementary desorption condition ($-15 \text{ J kg}^{-1} \psi$) was tested for beech wood.

Figure 1 shows that the loss of MC between full saturation and $-15 \text{ J kg}^{-1} \psi$ was 33% for beech. In the case of the tropical hardwoods, the loss of MC between full saturation and $-100 \text{ J kg}^{-1} \psi$ was 11% for congona and 15% for cachimbo. In terms of mass units, this corresponds to a loss of liquid water of 4.95 g for beech, 1.65 g for congona and 2.13 g for cachimbo. This water would have occupied a volume within the wood specimen of about 21% for beech, 7% for congona and 9% for cachimbo (mean volume of the specimens at 12% EMC was 24 cm^3). This water would have been removed from the larger capillaries, especially the vessel lumina. According to anatomical results obtained from matched samples, the proportion of vessel lumina within the total wood volume was of 25% for beech, 6% for congona and 8% for cachimbo (Almeida and Hernández 2006b). Table 1 shows that at $-15 \text{ J kg}^{-1} \psi$ capillaries with radius larger than $9.6 \mu\text{m}$ are already empty (at $-100 \text{ J kg}^{-1} \psi$ this size is of $1.44 \mu\text{m}$). The tangential radius of vessel elements was of $20.2 \mu\text{m}$ for beech, $47.5 \mu\text{m}$ for congona and $68.9 \mu\text{m}$ for cachimbo (Almeida and Hernández 2006b). Since no tyloses or other deposits into the vessel lumina were observed in the samples studied, it is apparent that the majority of vessel elements were already empty at this stage of desorption.

The boundary desorption curves of congona and cachimbo dropped greatly at different ranges of ψ values (Fig. 1). Congona lost 62% of MC between -100 and $-700 \text{ J kg}^{-1} \psi$ while cachimbo lost 38% of MC between -100 and $-300 \text{ J kg}^{-1} \psi$. In terms of mass units, this corresponds to a loss of liquid water of 8.64 g for congona and 5.38 g for cachimbo. This water would have occupied a volume within the wood specimen of about 36% for congona and 22% for cachimbo (mean volume of the specimens at 12% EMC was 24 cm^3). The proportion of fiber lumina and axial parenchyma within the total wood volume of these two species was 31% for congona and 27% for cachimbo (Almeida and Hernández 2006b). These similarities between anatomical and sorption results indicate that the boundary longitudinal drainage occurs first in the vessels, followed by the fiber lumina and axial parenchyma.

Figure 1 shows that the drainage curve of cachimbo presented a plateau between -300 and $-700 \text{ J kg}^{-1} \psi$, which indicates that openings controlling the retention and flow of water are scarce within these ψ values. For congona, the plateau corresponded rather to ψ values between -700 and $-2,000 \text{ J kg}^{-1}$. Below the ψ region of these plateaus, the water remaining in wood would be localized in capillaries having a radius equal to or smaller than about $0.21 \mu\text{m}$

(cachimbo) and $0.072 \mu\text{m}$ (congona) (Table 1). This would correspond to the transition between the drainage of the fiber cavities and that of the cell walls and ray parenchyma lumina. Almeida and Hernández (2006a) compared the water drainage of yellow birch and sugar maple and observed a plateau between -700 and $-2,000 \text{ J kg}^{-1} \psi$ for yellow birch and between -300 and $-2,000 \text{ J kg}^{-1}$ for sugar maple. As concluded for these two temperate species, an important part of the liquid water remaining below these plateaus could be entrapped in the ray parenchyma cells as noted by Hart (1984).

As discussed before, beech wood lost a great quantity of MC between the full saturation and $-100 \text{ J kg}^{-1} \psi$ (Fig. 1). According to the desorption conditions tested, an intermediate plateau is absent in its boundary drainage curve. For softwood species, Fortin (1979) and Tremblay et al. (1996) also observed a drainage curve without an intermediate plateau. A more uniform distribution of pore openings may explain the absence of a plateau for these species. Such results confirm that at high humidities, the EMC– ψ relationship is highly dependent on species.

The boundary desorption curves of the three species nearly meet below 76% RH (Fig. 1). The same was observed for yellow birch and sugar maple woods (Almeida and Hernández 2006a). This was expected given that desorption of liquid water at this level of RH is almost achieved. More precisely, Hernández (1983) reported that loss of liquid water for sugar maple will be accomplished at about 63% RH, which corresponds to nearly 14% EMC. In general, desorption of bound water is quite similar for temperate neutral woods as beech. The congona and cachimbo hardwoods exhibited also a similar behavior, which probably indicates that their proportion of wood extractives is low (Hernández 2006).

For congona and cachimbo woods, it was not possible to determine the FSP by the adsorption over distilled water method (Table 1). Equilibrium was not reached because condensation of water occurred simultaneously with bound water adsorption (Hernández 2006). For this reason, the FSP was determined by the volumetric shrinkage intersection point method. In this method, the FSP is defined as the MC of wood at which the extended straight linear portion of the shrinkage–EMC curve intersects the line of zero shrinkage. For this estimation, only volumetric shrinkage values obtained between 33 and 76% RH were used. This was done because of the non-linearity of the shrinkage–EMC curve at low moisture contents (Kelsey 1956) and the effect of the hysteresis at saturation on shrinkage at high moisture contents (Hernández and Bizoň 1994). The estimated FSP were 31, 24 and 25%, for beech, congona and cachimbo, respectively. The FSP values estimated by the volumetric shrinkage intersection point method (actual FSP) are used in the discussion that follows.

Wood shrinkage–EMC relationships

The relationships between the EMC and the radial, tangential and volumetric shrinkages of the three hardwoods are shown in Fig. 2. Even though

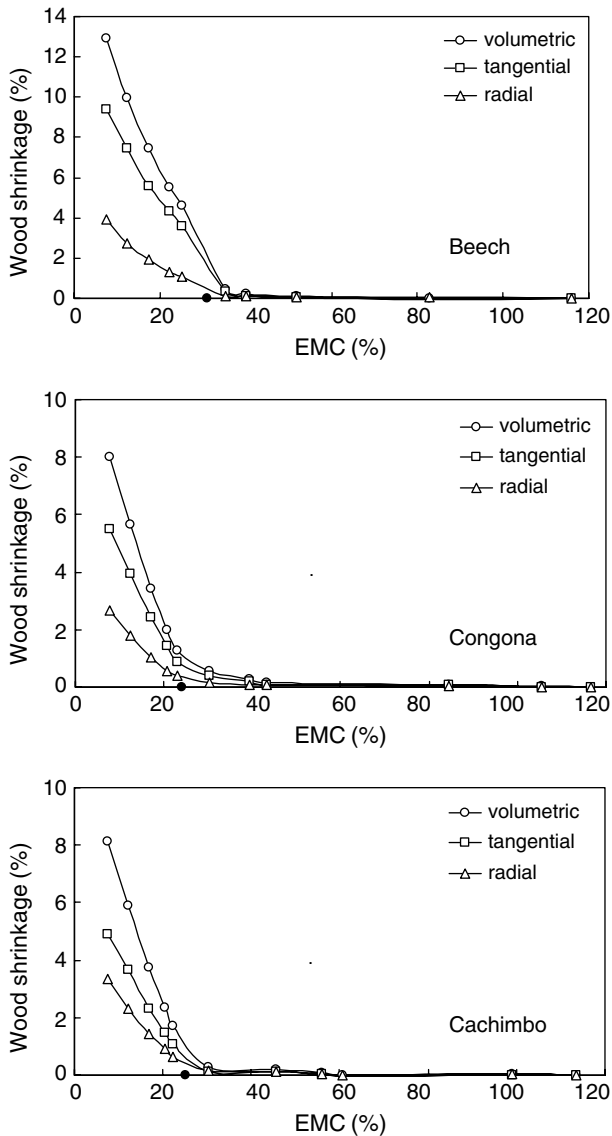


Fig. 2 Shrinkage of beech, congona and cachimbo hardwoods as a function of the EMC at 25°C. Filled circle represents the FSP estimated by the volumetric shrinkage intersection method

the three species studied had a similar basic wood density, beech wood exhibited a higher shrinkage than the tropical hardwoods. The volumetric shrinkage of congona and cachimbo were very similar. However, cachimbo showed a lower T/R ratio than congona. Based on these results, cachimbo would be the more dimensional stable wood, followed by congona and finally, beech wood.

The actual FSP of each species is also depicted in Fig. 2 and it is observed that radial, tangential and volumetric shrinkages started before the bulk FSP of wood was reached. In order to determine the EMC at which shrinkage starts to take place, the difference between the dimensions at full moisture saturated state and those at each EMC studied were calculated. This was made for the tangential and radial dimensions of samples. Since the dimensions at full moisture saturation and at each EMC studied were taken on the same specimen, a paired *t*-test (one-tail) was performed (Statistical Analysis System 2002–2003). This test determined if changes in dimensions between these two MCs were statistically larger than zero at the 0.01 probability level. The results of the paired *t*-tests indicating the EMC at which shrinkage begins to take place in both principal directions of wood are shown in Table 2.

The EMC at which shrinkage was larger than zero varied among wood species (Table 2). This was expected since water drainage at high moisture contents is highly dependent on wood structure. Table 2 shows that in beech wood tangential and radial shrinkages started at 40.2% EMC, which corresponds to $-2,000 \text{ J kg}^{-1} \psi$. Since the actual FSP for beech was estimated to be 31%, shrinkage started before the FSP was reached. It is apparent that, even at equilibrium, loss of bound water within the cell walls provokes shrinkage of wood before all liquid water has evaporated. This implies that about 9% MC in liquid form is still retained in the wood when shrinkage of beech starts taking place at $-2,000 \text{ J kg}^{-1} \psi$ (40–31% EMC). In terms of mass units, this corresponds to 1.38 g of liquid water that would have occupied a volume of about 6% within the wood specimen (mean volume of the specimens at 12% EMC was 24 cm^3). This remaining liquid water could be entrapped in the ray elements, given that these wood elements are considered as the least permeable flow path in hardwoods (Siau 1984, 1995). This entrapped water could in fact partially fill the 12% volume of ray tissue measured on matched

Table 2 Paired *t*-test results of the difference in dimensions of specimens after full moisture saturation and at a given EMC for the three species

Wood species	EMC ^a (%)	Tangential direction ^b				Radial direction ^c			
		T_{FS} (mm)	T_{EMC} (mm)	Diff <i>T</i> (mm)	<i>t</i> Value	R_{FS} (mm)	R_{EMC} (mm)	Diff <i>R</i> (mm)	<i>t</i> Value
Beech	40	65.139	65.066	0.073 (0.006) ^d	11.73**	20.636	20.610	0.026 (0.004)	6.22**
Congona	43	62.733	62.690	0.043 (0.008)	5.58**	20.463	20.445	0.017 (0.003)	5.22**
Cachimbo	56	62.931	62.897	0.034 (0.005)	7.42**	20.629	20.622	0.007 (0.003)	2.66**

^aEquilibrium moisture content where Diff *T* (difference between T_{FS} and T_{EMC} dimensions) and Diff *R* (difference between R_{FS} and R_{EMC} dimensions) were statistically higher than zero

^bAverage of 20 measurements: T_{FS} tangential dimension at full saturation, T_{EMC} tangential dimension at EMC

^cAverage of 20 measurements: R_{FS} radial dimension at full saturation, R_{EMC} radial dimension at EMC

^dValues between parentheses represent the standard error

**Significant at the 1% probability level

specimens of beech wood by Almeida and Hernández (2006b). The entrapment of liquid water in ray tissue reported by Hart (1984) for hickory and oak adds further support to this hypothesis. Menon et al. (1987) studied the water location during the drying of Douglas fir and western red cedar using proton magnetic resonance techniques. Under unequilibrated conditions, they observed that liquid water remained in the ray and tracheid compartments when bound water begins to leave the cell walls. The liquid water was all lost when the MC reached values as low as 9%. According to Skaar (1988), the presence of water-soluble materials in the cavities of parenchyma cells may reduce the humidity at which moisture may condense.

For the tropical hardwoods, shrinkage was statistically different from zero at 43% EMC for congona ($-700 \text{ J kg}^{-1} \psi$) and at 56% EMC for cachimbo ($-700 \text{ J kg}^{-1} \psi$). These EMCs are also larger than the actual FSP for these species (24% EMC for congona and 25% for cachimbo). About 19% MC in liquid form is still retained in congona wood when shrinkage starts taking place at $-700 \text{ J kg}^{-1} \psi$ (43–24% EMC). For cachimbo, 31% MC in liquid form is still retained in the wood when shrinkage starts taking place at $-700 \text{ J kg}^{-1} \psi$ (56–25% EMC). In terms of mass units, this corresponds to 2.81 g (congona) and 4.36 g (cachimbo) of liquid water that would have occupied a volume of about 12% (congona) and 18% (cachimbo) within wood specimen (mean volume of the specimens at 12% EMC was 24 cm^3). The volume of ray tissue was 17 and 21%, for congona and cachimbo, respectively (Almeida and Hernández 2006b). As for beech wood, the entrapped water appears to be located principally in the ray tissue.

The presence of the entrapped water on the less permeable wood elements can also be explained by the invasion percolation theory. During the drainage, it is possible that clusters of water-filled cells are separated from the continuous water phase (surrounded by air). This water cannot escape and thus air cannot displace it (Berkowitz and Ewing 1998).

Hernández and Pontin (2006) observed that shrinkage of huayruro wood started at a very high EMC (77%). This hardwood exhibits a high proportion of axial parenchyma within wood volume (34%) and the beginning of dimensional changes at a higher EMC compared to the other species could be due to a localized collapse on this tissue. According to these authors, the hypothesis of cell-wall shrinkage from bound water loss taking place in presence of liquid water appears to be more plausible for homogeneous hardwoods as the species studied in the present work. It was hence postulated that these two mechanisms could occur simultaneously in heterogeneous hardwoods.

Figure 2 also shows that below about 20% EMC the curves of volumetric shrinkage have a straight trend. Barkas (1938) observed this behavior in beech wood and concluded that below 20% EMC, the graph is sufficiently straight to justify the assumption of rectilinear shrinkage in dealing with practical problems. However, one must consider the non-linearity of the shrinkage–EMC relationship at low EMCs (Kelsey 1956). The non-linearity of this relationship above 20% EMC is attributed to the effect of the hysteresis at

saturation as previously discussed. Such limitations must be considered in models used to adjust the shrinkage and density of wood as a function of its MC.

Tangential compression strength–EMC relationships

The relationship between EMC and the compliance coefficient in the tangential direction of wood (s_{33}) of the three species is shown in Fig. 3. This

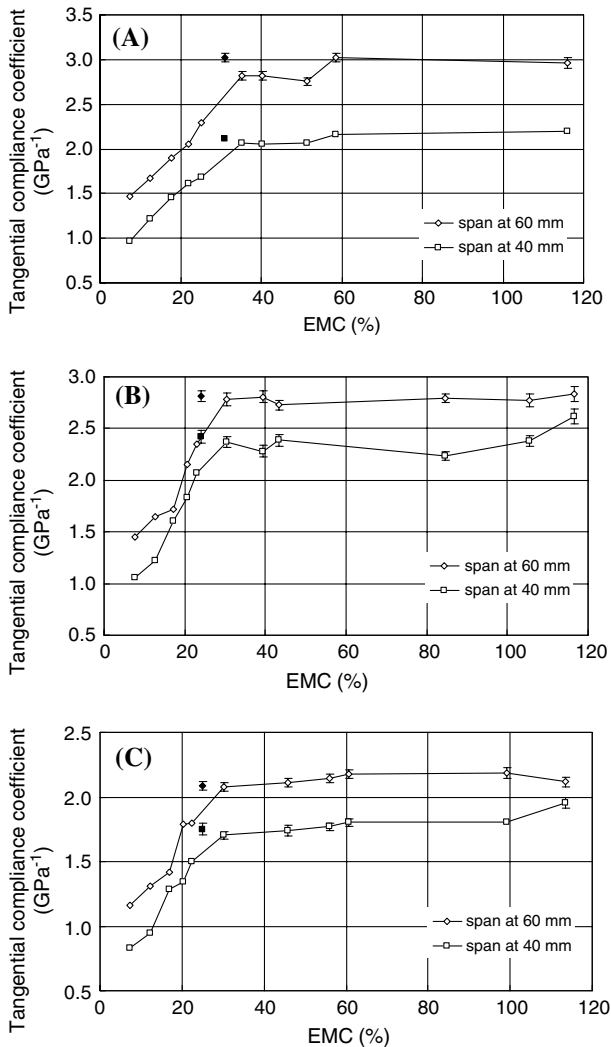


Fig. 3 Compliance coefficients s_{33} in tangential compression of beech (a), congona (b) and cachimbo (c) hardwoods as a function of the EMC. The symbols filled diamond and filled square represent the FSP estimated by the volumetric shrinkage intersection method (standard errors are shown only when they exceed the symbol size)

figure displays the compliance coefficient measured over the central part of the sample (40 mm), as well as the coefficient estimated over its entire length.

As observed in other studies (Hernández 1993; Hernández and Bizoň 1994; Almeida and Hernández 2006a), the curves obtained in the central part and over the entire length show that there is a heterogeneous distribution of the strain inside the wood specimen. The entire compliance coefficient s_{33} was on average 37% (beech), 17% (congona) and 21% (cachimbo) higher than the median compliance coefficient.

The effect of the hysteresis at saturation on the tangential compliance coefficient of the three species can also be observed in Fig. 3. This is apparent when comparing the s_{33} obtained at the actual FSP with the s_{33} obtained on the boundary desorption curve at a similar EMC (31% for beech, 24% for congona and 25% for cachimbo). The difference between the s_{33} values obtained at this EMC condition was 14% (beech), 15% (congona) and 9% (cachimbo) for the strains evaluated over the entire length of the specimens. This difference between the s_{33} values was 10% for beech, 13% for congona and 10% for cachimbo for the strains evaluated in the central part of the specimens. However, compliance coefficient values for the three species showed a greater variation at high EMCs (Fig. 3). As a result, the initial EMC at which the s_{33} property starts to change could not be determined. A similar variation was also observed in a previous work with yellow birch wood (Almeida and Hernández 2006a).

For sugar maple wood, Hernández and Bizoň (1994) reported a difference of about 10% between the compliance coefficient obtained at the FSP (31% EMC) and that measured at the maximum MC (full saturation). This difference was attributed to the saturation treatment used to attain the maximum MC, where samples of 14% EMC were directly immersed in distilled water. For yellow birch, the saturation treatment was performed in three steps, which resulted in statistically equal values of s_{33} at the FSP (29% EMC) and at the maximum MC (Almeida and Hernández 2006a). In the present study, the specimens were also saturated in three steps, which generally resulted in statistically equal values of s_{33} at the FSP and at the maximum MC for the three species. Only the strain measured on the central part of the specimen for congona and cachimbo woods showed higher values at the maximum MC. This difference could be explained by the large variation obtained in the measurement of strain for these two tropical hardwoods. However, in general these results show that a mild saturation effectively avoids internal defects in wood samples and confirmed the suggestions given by Naderi and Hernández (1997).

General discussion

As noted for shrinkage, gain in tangential strength for the three woods started before the FSP was reached as a result of the loss of bound water in presence of liquid water (Figs 2, 3). Such changes in physical properties started at 42.5% EMC for sugar maple (Hernández and Bizoň 1994) and at about 41%

EMC for yellow birch (Almeida and Hernández 2006a). In the present work, wood species presenting different structure showed that changes in wood properties began at different EMC values: at nearly 40% EMC for beech, 43% EMC for congona and 56% EMC for cachimbo. These values do not correspond to any abrupt transition from bound water to liquid water as currently stated. The results of this study confirm that during desorption a region exists where the loss of bound water takes place in the presence of liquid water. The range of EMC of this region depends on the size distribution of wood capillaries and, as a result, this varied among wood species.

Summary and conclusions

One temperate [beech (*F. grandifolia*)] and two tropical hardwoods [congona (*B. alicastrum*) and cachimbo (*C. domestica*)] were submitted to moisture desorption experiments at 25°C. Special attention was paid to the fiber saturation zone. Once equilibrium was reached, shrinkage measurements and tangential compression tests were undertaken. The results of these tests lead to the following main conclusions:

1. At equilibrium, the radial, tangential shrinkage and, consequently, the volumetric shrinkage begin well above the actual FSP for the three species studied. The EMC at which shrinkage begins to take place varied among species.
2. At equilibrium, the moisture content affects the tangential compliance coefficient beyond the actual FSP for the three species studied.
3. In desorption phase, loss of bound water begins at nearly 40% EMC for beech, 43% EMC for congona and 56% EMC for cachimbo in the presence of liquid water. The amount of liquid water that remained in the wood volume when the shrinkage began was estimated to be 6% for beech, 12% for congona and 18% for cachimbo. This amount varied among wood species and depended on the wood microstructure.

Acknowledgments The authors are grateful to Professor Yves Fortin for valuable suggestions and help. They are also grateful to Exportimo S.A.C. (Peru) for providing congona and cachimbo specimens. This research was supported by the National Council for Scientific and Technological Development of Brazil (CNPq) and the Natural Sciences and Engineering Research Council of Canada.

References

- Almeida G, Hernández RE (2006a) Changes in physical properties of yellow birch below and above the fiber saturation point. *Wood Fiber Sci* 38(1):74–83
- Almeida G, Hernández RE (2006b) Influence of the pore structure of wood on moisture desorption at high relative humidities (unpublished)
- Barkas WW (1938) Recent work on the moisture in wood in relation to strength and shrinkage. His Majesty's Stationery Office, London

- Berkowitz B, Ewing RP (1998) Percolation theory and network modeling applications in soil physics. *Surveys in Geophysics* 19:23–72
- Bodig J, Jayne BA (1982) *Mechanics of wood and wood composites*. Van Nostrand Reinhold, New York
- Cloutier A, Fortin Y (1991) Moisture content–water potential relationship of wood from saturated to dry conditions. *Wood Sci Technol* 25:263–280
- Defo M, Fortin Y, Cloutier A (1999) Moisture content–water potential relationship of sugar maple and white spruce wood from green to dry conditions. *Wood Fiber Sci* 31(1):62–70
- Fortin Y (1979) Moisture content–water potential relationship and water flow properties of wood at high moisture contents. Ph.D. Thesis, University of British Columbia, Vancouver
- Goulet M, Hernández RE (1991) Influence of moisture sorption on the strength of sugar maple wood in tangential tension. *Wood Fiber Sci* 23(2):197–206
- Griffin DM (1977) Water potential and wood-decay fungi. *Ann Rev Phytopathol* 15:319–329
- Hart CA (1984) Relative humidity, EMC, and collapse shrinkage in wood. *Forest Prod J* 34(11/12):45–54
- Hernández RE (1983) Relations entre l'état de sorption et la résistance du bois d'érable à sucre en traction tangentielle. M.Sc. Thesis, Département d'exploitation et utilisation des bois, Université Laval, Québec
- Hernández RE (1993) Influence of moisture sorption on the compressive properties of hardwoods. *Wood Fiber Sci* 25(1):103–111
- Hernández RE (2006) Moisture sorption properties of hardwoods as affected by their extraneous substances, wood density and interlocked grain (unpublished)
- Hernández RE, Bizoñ M (1994) Changes in shrinkage and tangential compression strength of sugar maple below and above the fiber saturation point. *Wood Fiber Sci* 26(3):360–369
- Hernández RE, Pontin M (2006) Shrinkage of three tropical hardwoods below and above the fiber saturation point. *Wood Fiber Sci* (in press)
- Kelsey KE (1956) The shrinkage intersection point—its significance and the method of its determination. *Forest Prod J* 6:411–416
- Menon RS, Mackay AL, Hailey JRT, Bloom M, Burgess AE, Swanson JS (1987) An NMR determination of the physiological water distribution in wood during drying. *J Appl Polym Sci* 33:1141–1155
- Naderi N, Hernández RE (1997) Effect of a re-wetting treatment on the dimensional changes of sugar maple wood. *Wood Fiber Sci* 29(4):340–344
- SAS Institute (2002–2003) SAS 9.1 ed. SAS Institute, Inc., Cary
- Siau JF (1984) *Transport processes in wood*. Springer, Berlin Heidelberg New York
- Siau JF (1995) *Wood: influence of moisture on physical properties*. Virginia Polytechnic Institute and State University, VA
- Skaar C (1988) *Wood–water relations*. Springer, Berlin Heidelberg New York
- Sliker A (1978) Strain as a function of stress, stress rate, and time at 90° to the grain in sugar pine. *Wood Sci* 10(4):208–219
- Stevens WC (1963) The transverse shrinkage of wood. *Forest Prod J* 13(9):386–389
- Stone JE, Scallan AM (1967) The effect of component removal upon the porous structure of the cell wall of wood. II. Swelling in water and the fiber saturation point. *Tappi* 50(10):496–501
- Tiemann HD (1906) Effect of moisture upon the strength and stiffness of wood. USDA Forest Service, Bulletin 70
- Tremblay C, Cloutier A, Fortin Y (1996) Moisture content–water potential relationship of red pine sapwood above the fiber saturation point and determination of the effective pore size distribution. *Wood Sci Technol* 30:361–371
- U.S. Department of Agriculture, Forest Service, Forest Products Laboratory (1974) *Wood handbook: wood as an engineering material*. USDA Agric. Handb. 72. Rev. USDA, Washington